I. SUPPLEMENTARY NOTES. CLONING RATE AND PROBABILITY DISTRIBUTION FUNCTION

A. Evolution of walkers

Hamilton's equations of motion with noise: $\mathbf{q} = \mathbf{p}$, $\dot{\mathbf{p}} = -\nabla V(\mathbf{q}) + \sqrt{\epsilon}\eta(t)$ can be written in a compact form:

$$\dot{x}_i = -\omega_{ij}\frac{\partial \mathcal{H}}{\partial x_j} + D_i\eta_i \tag{1}$$

where $\mathbf{x} = (q_1 \cdots q_N, p_1 \cdots p_N)$, $D_i = (0 \cdots 0, 1 \cdots 1)$, $\omega = \begin{pmatrix} 0 & -1 \\ 1 & 0 \end{pmatrix}$ and repeted indices are summed over. The divergence of nearby trajectories is measured by the Lyapunov vector $\mathbf{u}$ which evolves as

$$\dot{u}_i = -A_{ij}u_j \qquad \text{where} \qquad A_{ij} = \omega_{ik}\frac{\partial^2 \mathcal{H}}{\partial x_k \partial x_j} \tag{2}$$

In terms of the unit vector $\mathbf{v} = \frac{\mathbf{u}}{|\mathbf{u}|}$, the norm of $\mathbf{u}$ is given by

$$|\mathbf{u}(t)| = |\mathbf{u}(0)|e^{-\int_0^t v_i A_{ij} v_j \mathrm{d}t} \tag{3}$$

while $\mathbf{v}$ evolves as

$$\dot{v}_i = -A_{ij}v_j + v_k A_{kl} v_l v_i \tag{4}$$

The generating function of the largest Lyapunov exponent at time t consequently reads

$$\langle e^{\alpha\lambda t}\rangle_{\text{traj.}} = \langle e^{-\alpha\int_0^t v_i A_{ij} v_j \mathrm{d}t}\rangle_{\text{traj.}} \tag{5}$$

where the average is over trajectories given by (1) and (4), and over the noise realisations. Using standard methods, this average can be written

$$\langle e^{\alpha\lambda t}\rangle_{\text{traj.}} = \int \mathrm{d}\mathbf{x}_t \mathrm{d}\mathbf{v}_t \quad e^{-t\left(H_{FP} + \alpha v_i A_{ij} v_j\right)} P_0(x_0, v_0) \tag{6}$$

where P_0 is the initial probability distribution and $(\mathbf{x}_t, \mathbf{v}_t)$ is the end point of the trajectories. The operator H_{FP} reads

$$H_{FP} = -\frac{\epsilon}{2}\frac{\partial^2}{\partial p_i^2} + p_i\frac{\partial}{\partial q_i} - \frac{\partial V(q)}{\partial q_i}\frac{\partial}{\partial p_i} - \frac{\partial}{\partial v_i}\left(A_{ij}v_j - v_k A_{kl} v_l v_i\right) \tag{7}$$

Equation (7) corresponds to an evolution:

$$\frac{\partial P}{\partial t} = -(H_{FP} + \alpha v_i A_{ij} v_j)P \tag{8}$$

It does not conserve probability:

$$\int \mathrm{d}\mathbf{x}\mathrm{d}\mathbf{v}\frac{\partial P}{\partial t} = -\alpha \int \mathrm{d}\mathbf{x}\mathrm{d}\mathbf{v}\ \ v_i A_{ij} v_j P \tag{9}$$

This simply says that if one represents $P(t)$ by a distribution of walkers, each one is cloned at every time step with a rate $-\alpha A_{ij} v_i v_j$, nothing but α times the stretching rate of $|\mathbf{u}(\mathbf{t})|$.

Clearly this derivation is not restricted to Hamiltonians of the form $p^2/2 + V(q)$ and is valid also for the time dependent case. Furthermore, maps like the standard map can always be written as a continuous time dependent Hamiltonian evolution:

$$\begin{aligned} &\dot{q} = 0 \qquad \dot{p} = \frac{k\delta}{2\pi}\sin(2\pi q) \qquad \text{for even time intervals} \\ &\dot{q} = p \qquad \dot{p} = 0 \qquad\qquad\qquad\ \ \text{for odd time intervals} \end{aligned} \tag{10}$$

and the derivation above applies to them.

B. Energy conserving noise

For a Hamiltonian of the form $\frac{\mathbf{p}^2}{2} + V(\mathbf{q})$, we implement an energy conserving stochastic dynamics by using a noise vector tangential to the energy surface:

$$\eta_i = \sum_j \left(\delta_{ij} - \frac{p_i p_j}{\mathbf{p}^2}\right)\rho_j \tag{11}$$

where ρ_j are independent white noises. When this equation is understood in the Stratonovich sense, it leads to microcanonical measure.

C. Legendre transform

Let us show at that time that by fixing α one can select – in the long time limit – trajectories with a desired Lyapunov exponent. By definition the generating function of the Lyapunov exponent is given by

$$\langle e^{\alpha\lambda t}\rangle_{\text{traj.}} = \int \mathrm{d}\lambda\ \rho(\lambda, t) e^{\alpha\lambda t} \tag{12}$$

where $\rho(\lambda, t)$ is the probability density of λ at time t. As is well-known, $\rho(\lambda)$ can be written for large times as a large deviation function: $\rho(\lambda, t) \simeq e^{tf(\lambda)}$. By saddle point evaluation one then gets

$$\langle e^{\alpha\lambda t}\rangle_{\text{traj.}} \simeq e^{t(\alpha\lambda^* + f(\lambda^*))} \tag{13}$$

where λ^* satisfies $f'(\lambda^*) = -\alpha$. The dominating orbits indeed have $\lambda = \lambda^*$, and $(\alpha\lambda^* + f(\lambda^*))$ is the typical cloning rate. Thus, from λ^* and the cloning rate, which are given by the algorithm, one can reconstruct $\rho(\lambda)$.

Probing rare physical trajectories with Lyapunov weighted dynamics

Julien Tailleur* and Jorge Kurchan†

Laboratoire PMMH (UMR 7636 CNRS;ESPCI;P6;P7)

10, Rue Vauquelin, 75231 Paris CEDEX 05, France

The transition from order to chaos has been a major subject of research since the work of Poincaré, as it is relevant in areas ranging from the foundations of statistical physics to the stability of the solar system[1, 2]. Along this transition, atypical structures like the first chaotic regions to appear, or the last regular islands to survive, play a crucial role in many physical situations. For instance, resonances and separatrices determine the fate of planetary systems[3, 4], and localised objects like solitons and breathers provide mechanisms of energy transport in nonlinear systems such as Bose-Einstein condensates and biological molecules[5, 6]. Unfortunately, despite the fundamental progress made in the last years, most of the numerical methods to locate these 'rare' trajectories are confined to low-dimensional or toy models, while the realms of statistical physics, chemical reactions, or astronomy are still hard to reach. Here we implement an efficient method that allows one to work in higher dimensions by selecting trajectories with unusual chaoticity. As an example, we study the Fermi-Pasta-Ulam nonlinear chain in equilibrium[6] and show that the algorithm rapidly singles out the soliton solutions when searching for trajectories with low level of chaoticity, and chaotic-breathers in the opposite situation. We expect the scheme to have natural applications in celestial mechanics and turbulence, where it can readily be combined with existing numerical methods.

Complex dynamical systems are generically chaotic: two nearby trajectories diverge exponentially with time, at a rate given by the Lyapunov exponent: $|\delta x(t)| = |\delta x(0)| \exp(t\lambda_{\text{orb.}})$. If chaoticity is sufficiently strong, almost every initial condition leads in the large-time limit

*Electronic address: tailleur@pmmh.espci.fr

†Electronic address: jorge@pmmh.espci.fr

to the same exponent $\lambda = \lim_{t\to\infty} \lambda_{\rm orb.}(t)$. Such an averaged description is not complete, as in many systems some trajectories will present atypically chaotic or regular behaviour extending (in the future or in the past) for very long periods – even forever – depending on their initial conditions.

A case in point is that of a planetary system [3, 4, 7]: of the possible sets of masses and orbital elements compatible with observational error, only some correspond to a situation not involving a planet ejection in the recent past or near future. Another example, to which we shall return below, is that of nonlinear media, where spatially localised soliton and 'breather' solutions (which have atypical Lyapunov exponents) are reached only from very specific initial conditions[5, 6].

In order to describe quantitatively the distribution of Lyapunov exponents of different trajectories, two closely related approaches, both inspired in thermodynamics, have been proposed in the past. In one approach, the sampling is over trajectories of fixed time and different initial conditions [8], while in the other the dynamics is perturbed with a small random noise, and the sampling is made over different noise realisations [9]. Lyapunov weighted dynamics (LWD) (a method proposed in the context of chemical reactions [10, 11]) can be modified to practically implement both these approaches – although here for brevity we discuss only the latter (see 'Method'). A population of walkers evolves in phase space with Hamiltonian dynamics, each one perturbed by an independent weak random force, which may be energy-conserving or not. The walkers carry with them a 'Lyapunov' vector that itself evolves as the separation between two nearby trajectories. After every time interval, walkers are cloned (or killed) with a rate proportional to (α times) the stretching rate of their Lyapunov vector. The end effect of the cloning is that orbits are now weighted according to their chaoticity.

A positive (negative) value of α tends to favour orbits with large (small) Lyapunov exponent. In fact, this procedure counts the trajectories with a weight $\exp(\alpha\lambda_{\rm orb.}t)$ (See supplementary notes). Within the formalisms mentioned above, α and λ are conjugate variables, just as inverse temperature and energy are in a thermodynamic problem: fixing α we obtain a typical value of λ, together with its probability and the trajectories that contribute.

In what follows we shall apply our method to several examples of increasing complexity.

Separatrices

Separatrices are the phase-space frontiers between regions with different dynamical behaviours. They play an important role because they are the cradle of chaos. In regular systems, walkers weighted with $\alpha = 1$ can be shown to converge there, and to populate them uniformly. This is illustrated in figure 1 for the simple example of a double well with potential energy $V(q) = p^2/2 + q^4 - 2q^2$. Particles can either librate within one of the wells, or oscillate between them. The separatrix is the curve emanating from the saddle point that limits these two regimes. Applying the dynamics with $\alpha = 1$, the clones slowly diffuse in energy because of the noise until they converge to the separatrix, where they multiply more favourably. Clones that subsequently diffuse away die without leaving offspring.

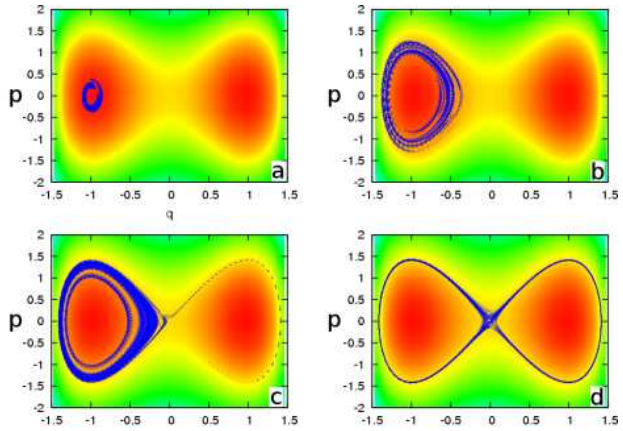

FIG. 1: **Convergence towards the separatrix.**

The color code represents the value of the energy. Starting in one well (**a**, $t \sim 3000$), the walkers first diffuse in energy (**b**, $t \sim 11450$) until they reach the separatrix (**c**, $t \sim 11725$), where they settle (**d**, $t > 12000$). Two thousands walkers were run with $\epsilon = 10^{-5}$ and $\alpha = 1$.

Let us now consider what happens as chaos sets in. We illustrate this with the classical example of the 'Standard Map':

$$p_{n+1} = p_n - \frac{k\delta}{2\pi}\sin(2\pi q) \qquad q_{n+1} = q_n + \delta p_{n+1} \tag{1}$$

It represents the evolution of a free rotor regularly kicked with a constant force of fixed orientation [2]. In the limit $\delta \to 0$, it reduces to the evolution of a pendulum, and is thus integrable. For $\delta > 0$, it becomes chaotic, the more so the larger δ and k. Applying the algorithm for $\alpha = 1$ close to integrability (figure 2.a), the walkers concentrate on the unstable

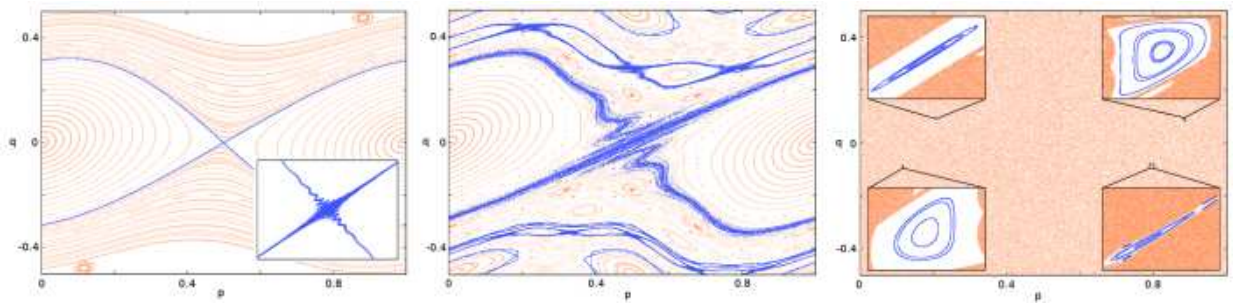

FIG. 2: **The Standard Map**

The standard map trajectories are represented in orange. In blue, a thousand walkers at time $T = 10,000$ evolving with $\epsilon = 10^{-16}$. **a)** Quasi-integrable case: $\delta = 0.41$, $k = 1$. The map is very slightly chaotic, and the walkers converge for $\alpha = 1$ to the homoclinic orbit emanating from the unstable fixed point. The inset is enlarged seventy-five times. **b** Secondary structures: $\delta = 1$, $k = 1$. Several separatrices are revealed, starting from different regular islands with $\alpha = 1$. **c** The last four regular islands in a strongly chaotic case [12]: $\delta = 1$, $k = 7.7$ $\alpha = -1$. The insets are zoomed between 25 times (bottom right) and 150 times (top) and are centered around: $(0.207; 0.09)$, $(0.883; 0.09)$, $(0.116; -0.09)$ and $(0.8; -.09)$.

manifold emanating from the fixed point, revealing the typical features of the homoclinic tangle. When chaos is increased — for larger δ — many secondary structures become apparent (figure 2.b). Around the main resonant island, a stochastic layer is now the most chaotic structure of the phase space, and will consequently be the favoured target of the walkers. Nevertheless, starting from a given configuration, the walkers first converge to the closest stochastic layer, where they stay for some time. In other words, chaotic layers are the metastable states of the $\alpha = 1$ dynamics.

For a strongly chaotic system, we may wish to explore hidden regular structures [12] lost in the chaotic sea. Choosing $\alpha = -1$, we bias the measure in favour of regular orbits, thus revealing the — otherwise invisible — last resonant islands (see figure 2.c).

Arnold Diffusion

An integrable Hamiltonian system has a constant of motion for every degree of freedom. The phase space is filled with invariant tori on which the motion is quasi-periodic, with frequencies $\omega_1 \cdots \omega_N$. Under a small perturbation, phase space is qualitatively unchanged, except for a chaotic region in the neighbourhood of 'resonances', defined as the points satis-

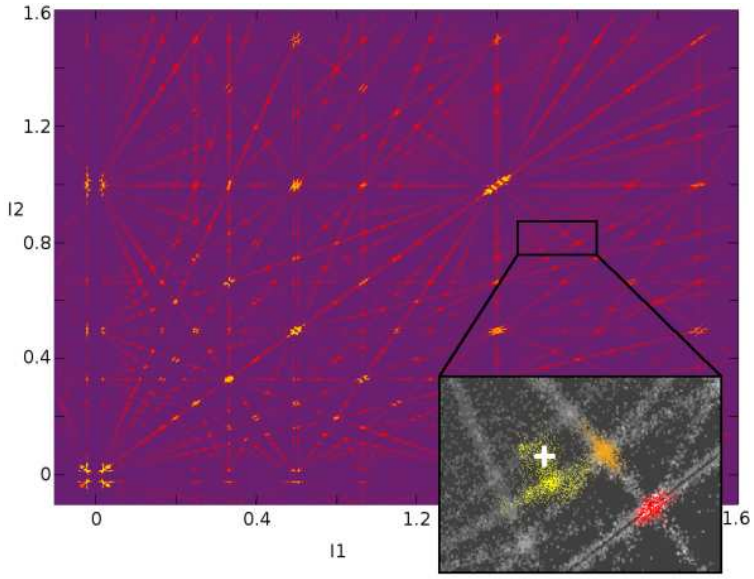

FIG. 3: **Arnold web and convergence.**

Arnold Web for the Hamiltonian (2) with $\mu = 10^{-3}$, very close to integrability. Lighter regions have stronger chaoticity. In the inset: the evolution of a set of clones in three successive times, starting from the point indicated by the white cross. Yellow for $0 < t < 160,000$, orange for $160,000 < t < 2,000,000$ and red for $2,100,000 < t < 2,200,000$. The large picture was composed by repeating the procedure shown in the inset for several initial conditions. Note that although the evolution of the clones resembles Arnold diffusion, it is in fact noise-driven, and hence orders of magnitude faster.

fying the Diophantine relation: $\sum n_i \omega_i = 0$ with n_i integer. In systems with more than two degrees of freedom, this 'chaotic web' leads to global diffusion in phase-space [1, 2]. This phenomenon, predicted by Arnol'd in 1964 [13], is called Arnol'd diffusion and the stochastic web is consequently called Arnol'd web. Localising such diffusive part of phase space is of great interest for many systems, for instance in synchrotron experiments [14], plasma physics or celestial mechanics. Laskar [15] developed a successful method, based on Fourier analysis, to map completely the regular part of phase-space. Here we are interested in going straight to the chaotic regions, which may be very thin and hard to find. Applying LWD with $\alpha > 0$, the walkers first diffuse in phase space thanks to the stochastic noise, until they reach chaotic structures, where they multiply and settle. As a benchmark, we constructed the Arnol'd web for the Hamiltonian [16]:

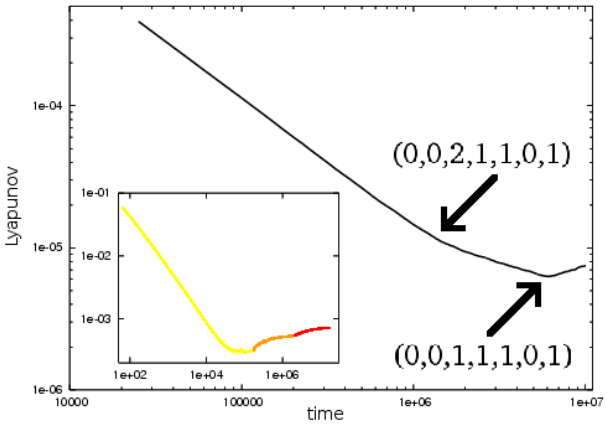

FIG. 4: **Finding resonances in higher dimensions.**

Main figure: a 6 degree of freedom system with Hamiltonian (2) and $\mu = 5.10^{-6}$, starting from a random initial condition. The two inflection points indicated by the arrows correspond to times at which the clones reached the resonances labeled $(n_1, n_2, n_3, n_4, n_5, n_6, n_7)$. In the inset: the same plot for the dynamics in the inset of figure 3; yellow, orange and red correspond to the same three times shown there.

$$\mathcal{H} = \sum_{i=1}^{N} \frac{p_i^2}{2} + p_{N+1} + \frac{\mu}{\sum_{i=1}^{N} \cos q_i + \cos t + N + 2} \tag{2}$$

Consider first the two-dimensional case $N = 2$. When $\mu = 0$, this Hamiltonian is integrable, and the resonance lines are given by $n_1 p_1 + n_2 p_2 = n_3$. For very small μ the chaotic set, shown in figure 3, is concentrated around the resonance lines. On the inset, one can see the path followed by the walkers that started in a random initial condition: they diffuse and settle in successive chaotic regions. The important point is that although the trajectory of the clones mimics Arnold diffusion, it happens in a timescale orders of magnitude shorter, as it is driven by noise. On the inset of figure 4 we show that each time the clones find a resonance there is an inflection in the finite-time Lyapunov exponent. Figures like 3 have been obtained in [16] by computing the finite-time Lyapunov exponents of trajectories starting in points on a grid in (p_1, p_2). Here, instead, we run LWD as in the inset, starting from several initial conditions.

In higher dimensions, the Arnold web is both difficult to represent and impossible to map exhaustively using a grid. There is no problem, however, in applying LWD as described above. To illustrate this, in figure 4 we show for the 6 degree of freedom version of (2) the

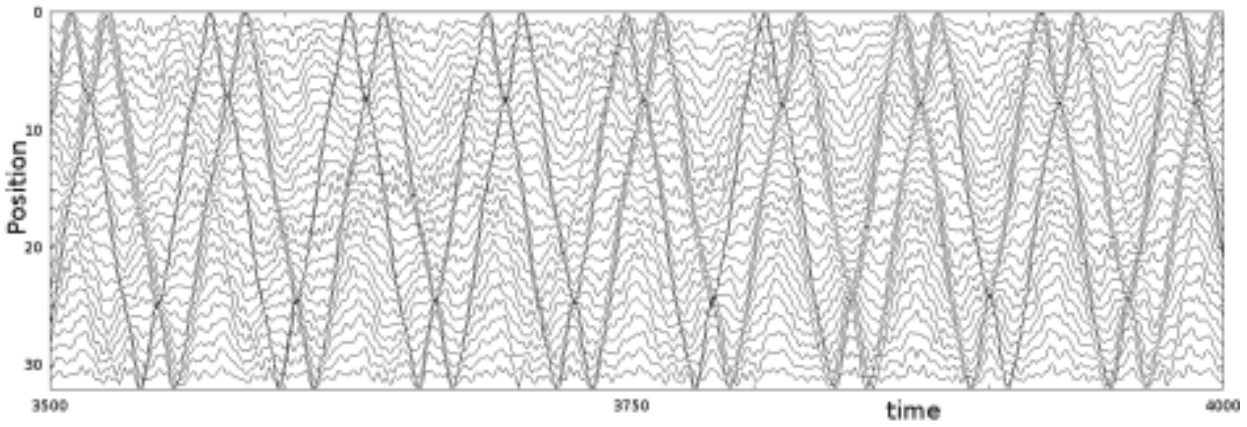

FIG. 5: **Finding solitons**

Energy-conserving ($E = 1$) dynamics of the Fermi-Pasta-Ulam chain with fixed ends, and strongly negative α, obtained starting from microcanonical equilibrium. The plot shows the position of the particles versus time. Several kinks bouncing from an end to the other of the chain are clearly visible. The Lyapunov exponent is half the typical value. (For clarity, the particles' average position has been arbitrarily displaced).

running-time evaluation of the clones' Lyapunov exponent starting from a random configuration. Using a separate programme, we have checked that the inflections indeed occured when the clones found the resonances indicated with arrows. Few-planet systems are clearly within reach, and LWD could be used to locate nearby chaotic trajectories in agreement with experimental data, in the spirit of [17].

Breathers and Solitons

As an example with many degrees of freedom, consider the Fermi-Pasta-Ulam chain, defined by the Hamiltonian:

$$H = \sum_i \left(\frac{1}{2} p_i^2 + \frac{1}{2}(x_i - x_{i+1})^2 + \frac{1}{40}(x_i - x_{i+1})^4 \right) \tag{3}$$

This chain is known to have localised soliton excitations, as well as the so-called 'chaotic breathers' [5, 6]. These excitations are unstable, but can be observed for some time starting from suitable initial conditions. Solitons configurations have atypically low chaoticity, while, perhaps more surprisingly, chaotic breathers are indeed very chaotic [6].

We have run an energy-conserving version of LWD on the chain starting from a microcanonical equilibrium configuration. The results, for an energy density $E = 1$, corresponding

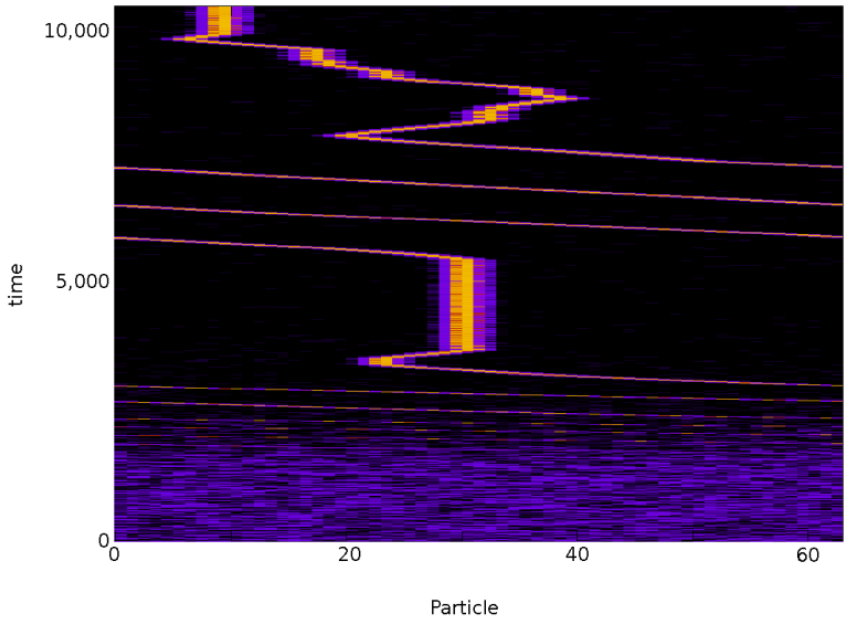

FIG. 6: **Finding a chaotic breathers.**
Energy-conserving (energy density $E = 1$) dynamics of the Fermi-Pasta-Ulam chain with periodic boundary conditions and large, positive α, starting from microcanonical equilibrium. The configuration evolves towards a single chaotic breather, whose Lyapunov is three times the one of a typical equilibrium trajectory. The colour code corresponds to the energy of the site.

to the 'transition region' [6], are shown in figures 5 and 6. When biasing to obtain a Lyapunov exponent three times larger than typical, we observe a chaotic-breather automatically emerging, thus showing that the large Lyapunov configurations are dominated by them. Conversely, constraining the Lyapunov exponent to be a half of the typical value results in a few-kink configuration, as is clearly visible in figure 5.

Conclusion

Let us conclude by suggesting that the special trajectories described here play the same role as the reaction paths in physical chemistry, whose efficient detemination is currently a field of intense activity [18]. In all cases one has to deal with events that are important but happen rarely, so they are best studied with a dynamics that is biased to enhance the probability of their occurrence – although of course one is ultimately interested in the properties of the true, physical dynamics.

Method A population of walkers with phase-space positions $\mathbf{x^a} \equiv (\mathbf{q^a}, \mathbf{p^a})$ is evolved

with the standard Hamiltonian dynamics $\dot{\mathbf{q}^{\mathbf{a}}} = \mathbf{p^a}$, $\dot{\mathbf{p}^{\mathbf{a}}} = -\nabla V(\mathbf{q^a}) + \sqrt{\epsilon}\eta(t)$, where η is a white noise of unit variance. Every clone has a 'companion' which starts a small distance $\delta\mathbf{x^a}(\mathbf{0})$ away, and evolves with the same noise. After a time interval δt, when the positions of clone and companion are $[(\mathbf{x}^a(\delta t), \mathbf{x}^a(\delta t) + \delta\mathbf{x}^a(\delta t)]$, and the separation ratio $p_a = \left(\frac{||\delta\mathbf{x}^a(\delta t)||}{||\delta\mathbf{x}^a(0)||}\right)$ *i)* their mutual separation is normalised $\delta\mathbf{x}^a \to \delta\mathbf{x}^a/p_a$, *ii)* if $(p_a)^\alpha > 1$ the clone a is copied (i.e. replaced by two clones) with probability $(p_a)^\alpha - 1$, while if $(p_a)^\alpha < 1$ it is killed with probability $1 - (p_a)^\alpha$. Each clone-companion pair subsquently evolves with a different noise realisation. An overall cloning rate is then applied to keep the population constant. In the energy-conserving variant, which we applied to the particle chain, the only difference is that the noise vector is tangential to the energy surface.

Acknowledgments

We would like to thank Giovanni Galavotti, Jacques Laskar, Stefano Ruffo and Sorin Tanase-Nicola for very useful discussions.

---

[1] Lichtenberg, A. L. and Lieberman M.A. *Regular and Chaotic Dynamics* (Springer 1992)

[2] Ott, E. *Chaos in dynamical systems* (Cambridge University Press, 1993)

[3] Laskar, J. A numerical experiment on the chaotic behaviour of the Solar System. *Nature* **338** 237-238 (1989)

[4] Murray N, Holman M, The role of chaotic resonances in the Solar System *Nature***410** (6830): 773-779 (2001)

[5] A. Trombettoni and A. Smerzi, Discrete Solitons and Breathers with Dilute Bose-Einstein Condensates *Phys. Rev. Lett.* **86**, 2353 - 2356 (2001).

[6] Cretegny T, Dauxois T, Ruffo S, Torcini A. Localization and equipartition of energy in the beta-FPU chain: Chaotic breathers *Physica* **D 121** 109-126 (1998)

[7] Murray N., Holman M. The origin of chaos in the outer solar system. *Science* **283**, 1877-1881 (1999)

[8] P. Grassberger, R. Badii and A. Politi, Scaling laws for invariant measures on hyperbolic and nonhyperbolic atractors, *J. Stat. Phys 51*, **135** (1988) 135 - 178

[9] R Benzi, G Paladin, G Parisi and A Vulpiani, Characterisation of intermittency in chaotic systems *J. Phys. A: Math. Gen.* **18** (1985) 2157-2165

[10] Tanase-Nicola S, Kurchan J Metastable states, transitions, basins and borders at finite temperatures *Journal of Statistical Physics* bf 116 1201-1245 (2004)

[11] Tailleur J, Tanase-Nicola S, Kurchan J Kramers equation and supersymmetry *Journal of Statistical Physics* bf 122 557-595 (2006)

[12] An apparently unrelated method to do this can be found in: J. H. E. Cartwright, M. O. Magnasco, O. Piro, and I. Tuval, Bailout Embeddings and Neutrally Buoyant Particles in Three-Dimensional Flows *Phys. Rev. Lett.* **89**, 264501 (2002)

[13] Arnold VI Instability of dynamical systems with many degrees of freedom *Doklady Akademii Nauk SSSR* **156** (1964)

[14] Robin, D., Steire, C., Laskar, J. & Nadolski, L. Global dynamics of the advanced light source revealed through experimental frequency map analysis. *Phys. Rev. Lett.* **85** 558-561 (2000)

[15] Laskar, J. Frequency-analysis for multidimensional systems - Global dynamics and diffusion. *Physica D* **67** 257-281 (1993)

[16] Froeschle, C., Guzzo, M., Legga, E. Graphical Evolution of the Arnold Web: From Order to Chaos. *Science* **289**, 2108-2110 (2000)

[17] Laskar J. Large-scale chaos in the solar-system *Astronomy and Astrophysics* **287** L9-L12 (1994)

[18] Bolhuis PG, Chandler D, Dellago C and Geissler PL, Transition path sampling: Throwing ropes over rough mountain passes, in the dark, *Annual Review of Physical Chemistry***53**: 291-318 (2002)